Far East Journal of Electronics and Communications

http://www.pphmj.com
http://dx.doi.org/10.17654/EC017050923
Volume 17, Number 5, 2017, Pages 923-939 **ISSN: 0973-7006**

INTERFERENCE OF COHERENT RADIATION IN A CRYSTALLINE TWO-COMPONENT LENS

A. Umbetov[1], M. Kozhahmet[1], G. Sabitbekova[1], M. Amirov[2], A. Hamit[2], G. Alieva[3], D. Karimova[1] and V. Uspanova[1]

[1]Mathematics and Physics Department
Arkalyk State Pedagogical Institute named after Ibrai Altynsarin
Arkalyk, Kazakhstan

[2]Department of Chemistry, Biology and Geography
Arkalyk State Pedagogical Institute named after Ibrai Altynsarin
Arkalyk, Kazakhstan

[3]Department of Informatics
Arkalyk State Pedagogical Institute named after Ibrai Altynsarin
Arkalyk, Kazakhstan

Abstract

Currently, uniaxial crystalline lenses become more widely used in laser technology and coherent optics. There are several types of crystalline lenses consisting of two lenses of a uniaxial crystal, which differ in the orientation of optical axes. These lenses are used in the mode of normal light incidence on the input face and carry out a shift between the wave fronts of ordinary and extraordinary beams at the output. The superposition of these waves at the output of crystalline lenses results in the occurrence of an interference pattern that can be used for a variety of purposes in laser polarized interferometers. A theory of the optical properties of crystals has been developed,

Received: February 16, 2017; Revised: May 14, 2017; Accepted: May 22, 2017
Keywords and phrases: interference, crystal coherence, lens, radiation laser, focus, raster, input, ordinary, unusual.

according to which the path of ordinary and extraordinary beams in crystalline lenses can be calculated for normal incidence of light on the input face of a crystalline lens. Crystalline lenses are used for releasing laser radiation in various laser measurement devices, obtaining a constant shift between the wave fronts of these beams, spatial encoding and decoding, spatial multiplying of optical signals and creating a controlled spatial filter. Many accurate measurements, the role of which is rapidly increasing in modern science and technology, are carried out by interference methods. The scope of application of interference devices has expanded through the creation of lasers and the development of electronics.

1. Introduction

The development of quantum electronics and coherent optics has greatly contributed to the increased use of various crystalline lenses in scientific, technological and industrial projects. Crystalline lenses help successfully to solve the problem of laser radiation control, control of amplitude, frequency, phase and polarization, creation of a continuous and discrete scanning of the laser beam, Q-switching and selection of optical resonator modes, management of the duration and form of laser pulses [1, 2]. Crystalline lenses are also used for creating controlled spatial filters [3-5]. On the basis of a crystalline lens, a number of laser polarization interferometric devices have been created [6], providing a high precision in the investigation of the quality of treatment of optical components [7], the geometric parameters of laser beams, the spatial correlation function of the laser radiation field and the degree of coherence [8].

The known calculations of the beam path in crystalline lenses are limited to the case of normal incidence of light on the front face of lenses and are conducted for each specific lens separately [15-18]. There is a method for calculating the beam path in birefringent prisms of the variable angle of splitting [19-21]. The theory of the propagation of electromagnetic waves in anisotropic crystals as well as the laws of reflection and refraction at the environmental interfaces were studied in research works of native and foreign authors [9-14, 22-35].

However, a rigorous calculation of the beam path in the system consisting of several anisotropic crystals results in cumbersome expressions, which are not suitable for engineering calculations and do not allow the general properties of crystalline lenses to be investigated [14]. Therefore, there is a need for an effective method to calculate the path of laser radiation in a crystalline lens, to describe the conditions of occurrence of interference patterns at the output of a crystalline lens and to study the possibility of using them in different laser polarized interferometers.

In this regard, the purpose of this paper is to present a detailed study of the properties of a crystalline optical lens made of the uniaxial crystal of an Icelandic spar with different orientations of the optical axes of crystals in lens components, to explore the conditions of occurrence of interference patterns at the output of a crystalline lens and to suggest the direction of their use.

2. Methods

The following tasks have been set and addressed in this paper:

- to develop an effective technique for calculating the path of laser radiation through a crystalline lens, suitable for the analysis of the properties of such systems and for engineering calculations;

- to carry out a comprehensive experimental study of a crystalline lens in the modes of splitting of polarized beams and interference between them and to investigate various cases of interference;

- to study the possibility of using crystalline lenses for the creation of new laser measurement devices.

3. Results and Discussion

The purpose of this research is to develop an effective technique for calculating the path of laser radiation through crystalline lenses.

The research objectives are as follows: to present a comprehensive experimental study of crystalline lenses, to analyze crystalline lenses in the modes of polarized beams as well as to give a detailed calculation of interference between polarized beams and to consider various cases of interference.

When the orthogonally polarized beams are shifted by the analyzer at the output of a crystalline lens (CL) (Figure 1(a)), a spatially non-localized interference pattern occurs in the place of the transposition of ordinary (o) and extraordinary (e) beams. The maximum contrast of the interference pattern is achieved, as known, at equal intensities of the mixed beams, which is achieved in turn by orienting the analyzer at an angle 45º to the planes of oscillation of the electric vector $\vec{E}$ for o- and e-beams. Below is the calculation of interference patterns (rasters), formed by two-component crystalline optical systems in parallel and divergent (or convergent) beams. Moreover, the focus is on the use of such crystalline optical systems in such devices as shearing interferometers.

In the general case, four waves are formed at the CL output. When the CL-incident beam is polarized in such a way that the direction of oscillation of its electric vector is defined by the unit vector $\overrightarrow{E_1}(0, 1, 0)$ (Figure 1(b)), at the CL output there appear (oo) and (oe) waves, which pass through CL-1 without being refracted. On the contrary, the beam with polarization $\overrightarrow{E_1}(1, 0, 0)$ is refracted and forms ordinary (eo) and extraordinary (ee) waves at the CL output.

Consider the interference pattern between (eo) and (ee) waves. The polarization of (eo) and (ee) waves at the CL output is shown in Figure 1.

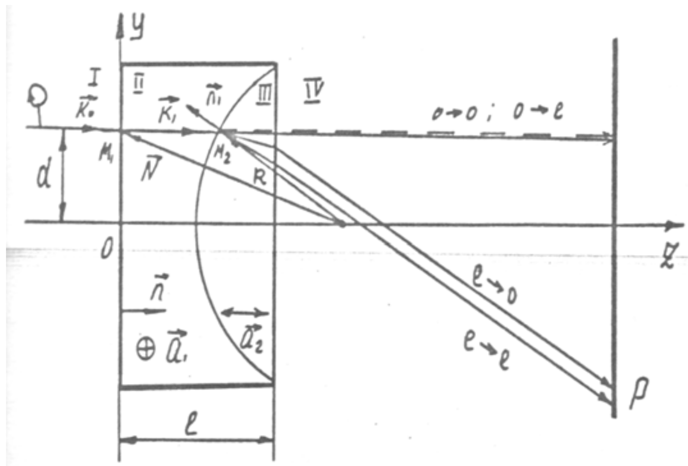

(a)

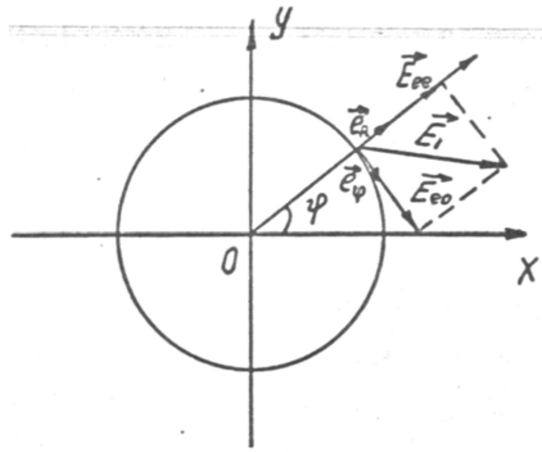

(b)

Figure 1. Polarization of (eo) and (ee) waves at the CL output in the collimated laser beam.

If the loss by internal scattering of the incident beam is neglected, then:

$$\vec{E}_{ee} = \vec{E}_1 \cos\varphi; \quad \vec{E}_{eo} = \vec{E}_1 \sin\varphi, \tag{1}$$

where $\vec{E}_1$ is the electric field intensity at the CL output.

In turn, the electric field intensity, according to Figure 1 and equation (1), can be expressed as follows:

$$\vec{E}_1 = \vec{e}_\rho E \cos\varphi e^{i\vec{k}_3^{ee}\vec{r}} + \vec{e}_\varphi E \sin\varphi e^{i\vec{k}_3^{eo}\vec{r}+ik\Delta l}, \quad (2)$$

where Δl is the path difference between o- and e-beams, $\vec{e}_\rho$ and $\vec{e}_\varphi$ are the unit vectors in the directions ρ and φ respectively and E is the preliminary field intensity.

If we go to the Cartesian coordinates, then:

$$\vec{e}_\rho = \vec{e}_x \cos\varphi + \vec{e}_y \sin\varphi;$$

$$\vec{e}_\varphi = \vec{e}_x \sin\varphi - \vec{e}_y \cos\varphi, \quad (3)$$

where $\vec{e}_x$, $\vec{e}_y$ are the unit vectors of the x- and y-axes.

Therefore:

$$\vec{E}_1 = \vec{e}_x\left(\cos^2\varphi e^{i\vec{k}_3^{ee}\vec{r}} + \sin^2\varphi e^{i\vec{k}_3^{eo}\vec{r}+ik\Delta l}\right)E$$

$$+ \vec{e}_y\left(\cos\varphi\sin\varphi e^{i\vec{k}_3^{ee}\vec{r}} + \sin\varphi\cos\varphi e^{i\vec{k}_3^{eo}\vec{r}+ik\Delta l}\right)E. \quad (4)$$

Let the analyzer have an oscillation along the x-axis:

$$|\vec{E}_{1x}|^2 = [\cos^2\varphi + \sin^2\varphi e^{ik\Delta l}]|E|^2$$

$$= E^2[(\cos^2\varphi + \sin^2\varphi\cos k\Delta l)^2 + \sin^4\varphi\sin^2 k\Delta l]$$

$$= E^2\left[1 - \sin^2 2\varphi\sin^2\left(k\frac{\Delta l'}{2}\right)\right], \quad (5)$$

where $\Delta L' = \Delta L + (\vec{k}_3^{eo} - \vec{k}_3^{ee})\vec{r}$.

Similarly, for the y-axis, we get:

$$|\vec{E}_{1y}|^2 = [1 - e^{ik\Delta l}]^2\cos^2\varphi\sin^2\varphi E^2 = E^2\sin^2 2\varphi\sin^2\left(k\frac{\Delta l'}{2}\right). \quad (6)$$

The path difference Δl for o- and e-beams on the paths M_1M_2, $M_2M_3^{ee}$ and $M_2M_3^{eo}$ (Figure 3) can be found through a direct calculation of the corresponding segments.

A simple calculation by the methods of analytic geometry gives the following expressions:

$$L_{M_1M_2} = -\left(h + R\frac{d^2}{2R^2}\right), \tag{7}$$

$$L_{M_2M_3^{eo}} = h\left\{1 + \frac{d^2}{2R^2}\left[\left(\frac{n_e}{n_o} - 1\right)^2 - \frac{R}{h}\right]\right\}, \tag{8}$$

$$L_{M_2M_3^{ee}} = h\left\{1 + \frac{d^2}{2R^2}\left[\frac{n_o^4}{n_e^4}\left(\frac{n_e}{n_o} - 1\right)^2 - \frac{R}{h}\right]\right\}. \tag{9}$$

Equations (7)-(9) make it possible to find the full path difference of o- and e-beams at the CL output

$$\Delta L = \Delta L_1 + \Delta L_2 = (n_o - n_e)\left(h + R\frac{d^2}{2R^2}\right) + hn_o\frac{d^2}{2R^2}\left(1 - \frac{n_o}{n_e}\right)^3\left(1 + \frac{n_o}{n_e}\right)$$

$$= (n_o - n_e)h + \left[(n_o - n_e)R + n_o h\left(1 - \frac{n_o}{n_e}\right)^3\left(1 + \frac{n_o}{n_e}\right)\right]\frac{d^2}{2R^2}. \tag{10}$$

Hence, for an Iceland spar, we obtain:

$$\Delta L = 0,17h + (0,17R - 0,01h)\frac{r^2}{R^2}. \tag{11}$$

For the plane of the screen, located at a distance from the CL, we have:

$$\Delta L = 0,17h + (0,17R - 0,01h)\left(\frac{F}{Z - F}\right)^2\frac{r^2}{R^2}, \tag{12}$$

where F is the focal distance, $r = \sqrt{x^2 + y^2}$ is the position (radial) of the point on the screen.

Thus, as seen from (6), at $\varphi = 0; \frac{\pi}{2}$, a dark field will be on the screen. At $\varphi = \frac{\pi}{4}$, the intensity varies according to the law:

$$|E_{1y}|^2 = |E|^2 \sin^2\left(k \frac{\Delta L'}{2}\right). \tag{13}$$

Since at the CL output two subsequent beams correspond to (eo) and (ee) waves, $\vec{k}_3^{eo} = \vec{k}_3^{ee}$, and it is possible to note:

$$\Delta L' = \Delta L.$$

The conventional signs of the interference maximum at $\varphi = \frac{\pi}{4}$ can be defined from (13) as follows:

$$k \frac{\Delta L}{2} = \left(S + \frac{1}{2}\right)\pi, \tag{14}$$

where $S = 0; \pm 1; \pm 2$.

Following from (14), with regard to formula (12), we obtain:

$$(0, 17R - 0, 01h)\left(\frac{F_{eo}}{Z - F_{eo}}\right)^2 \frac{x^2 + y^2}{R^2} = \left(S + \frac{1}{2}\right)\lambda - \Delta_1, \tag{15}$$

where $\Delta_1 = 0, 17h$.

Thus, the interference pattern for $|E_{1y}|^2$ has the form of concentric rings intersected by a dark cross (see Figure 2), and for $|E_{1x}|^2$-rings with a light cross (see Figure 2(b)). For $|E_{1y}|^2$ at $\varphi = \frac{\pi}{4}$, the locus of the points corresponding to the interference pattern by analogy with (15) can be written as:

$$(0, 17R - 0, 01h)\left(\frac{F_{eo}}{Z - F_{eo}}\right)^2 \frac{x^2 + y^2}{R^2} = S\lambda - \Delta_1. \tag{16}$$

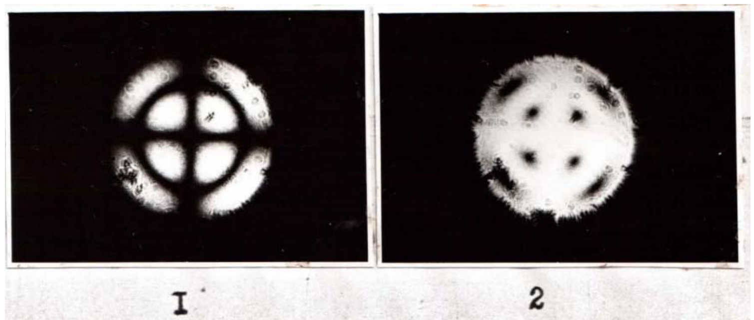

(a)

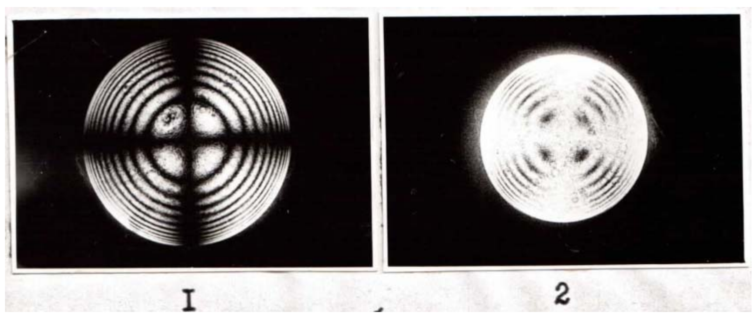

(b)

Figure 2. Interference rasters generated by the CL: (a) in a collimated laser beam at the input; (b) in a convergent laser beam at the input.

At the same time, $|E_{1y}|^2$ and $|E_{1x}|^2$ determine the intensity distribution in F_{eo} and F_{ee}, respectively. Indeed, the intensity distribution in the focus F_{ee} is given by the expression:

$$I_x \approx \int |E_{1x}|^2 ds = \int_0^{2\pi r_0} \int_0^{(\rho_0)} |E_{1x}|^2 d\varphi r(\rho) dr, \tag{17}$$

where $|E'_{1x}|^2 = \dfrac{F_{ee}}{Z - F_{ee}}$ is the intensity distribution on the screen located at a distance z from the CL, $ds = r(\rho) dr d\varphi$ is the element of area on the screen and ρ is the position (radial) of the point on the CL rear plane (Figure 3):

$$\rho = \sqrt{X_3^{ee^2} + Y_3^{ee^2}} = \rho_0\left[\frac{R-\sigma}{R}\left(\frac{n_e}{n_o}-1\right)+1\right]. \tag{18}$$

Hence

$$dr = \frac{Z - F_{ee}}{F_{ee}}\left[\frac{R-\delta}{R}\left(\frac{n_e}{n_o}-1\right)+1\right]d\rho_0. \tag{19}$$

Finally, with regard to (18) and (19), from (17) we obtain:

$$I_x \approx \int |E_{1x}|^2 ds$$

$$= \left(\frac{F_{ee}}{Z - F_{ee}}\right)^2 |E|^2 \int_0^{2\pi} \int_0^{r_0(\rho_0)} \left[1 - \sin^2 2\varphi \sin^2\left(k\frac{\Delta L}{2}\right)\right] d\varphi r(\rho) dr$$

$$= \frac{3}{4}\pi |E|^2 \left[\frac{R-\sigma}{R}\left(\frac{n_e}{n_o}-1\right)+1\right]^2 \rho_0^2$$

$$+ \frac{\lambda}{16\Delta L}|E|^2\left[\frac{R-\sigma}{R}\left(\frac{n_e}{n_o}-1\right)+1\right]^2 \sin[2k(\Delta L\rho_0^2 + B)], \tag{20}$$

where $B = \text{const}$.

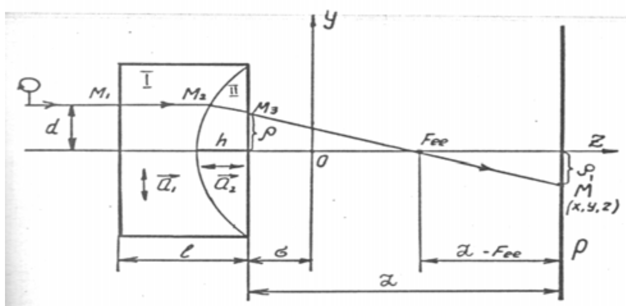

Figure 3. The scheme for calculating the distribution of light intensity in the focus F_{ee}.

Similarly, find the expression for the intensity distribution in the focus F_{eo}:

$$I_y \approx \int |E_{jy}|^2 ds$$

$$= \left(\frac{F_{eo}}{Z - F_{eo}}\right)^2 \int\limits_0^{2\pi r_0(\rho_0)} \sin^2 2\varphi \sin^2\left(k\frac{\Delta L}{2}\right) d\varphi r(\rho) dr$$

$$= \frac{\pi}{4}| E^2 |\left[\frac{R-\sigma}{R}\left(\frac{n_e}{n_o} - 1\right) + 1\right]^2 \rho_0^2$$

$$+ \frac{\lambda}{16\Delta L}| E |^2\left[\frac{R-\sigma}{R}\left(\frac{n_e}{n_o} - 1\right) + 1\right]^2 \sin[2k(\Delta L\rho_0^2 + B)]. \qquad (21)$$

The total intensity is given as

$$I = I_x + I_y = \pi\rho_0^2| E |^2\left[\frac{R-\sigma}{R}\left(\frac{n_e}{n_o} - 1\right) + 1\right]^2 = \pi\rho_0^2| E |^2. \qquad (22)$$

The second terms of the expressions (20) and (21) are small as compared with the first terms, and therefore, the intensity ratio in the focuses F_{ee} and F_{eo} is equal to:

$$\gamma = \frac{\int |E_{jx}|^2 ds}{\int |E_{jy}|^2 ds} = 3. \qquad (23)$$

The obtained result is in qualitative agreement with the experiment.

Next, consider the interference pattern between (oo) and (ee) beams at the CL output. As shown, the (oo)-beam passes through the CL without deviation, and the (ee)-beam passes through the focus determined according to the expression (12):

$$F_{ee} = \frac{R}{n_o - n_e} - \frac{n_o}{n_e^2} h,$$

where h is the height of the spherical segment, and the focal length is measured from the back face of the CL.

Take a point $M(x, y, z)$ on the screen and consider the incidence of (oo) and (ee) waves on this point. A simple calculation of the beam path within the accuracy of $\left(\frac{d}{R}\right)^2$ can show that the direction of the refracted e-beam is determined by the unit vector at the CL output (Figure 3), where

$$\overrightarrow{k_e} = (k_{ex}, k_{ey}, k_{ez}),$$

$$k_{ex} = \frac{\rho_1}{z - F_{ee}} \cos\varphi; \quad k_{ey} = \frac{\rho_1}{z - F_{ee}} \sin\varphi;$$

$$k_{ez} = \sqrt{1 - \left(\frac{\rho_1}{z - F_{ee}}\right)^2} \tag{24}$$

and in the area II within CL- by the vector $\vec{k}'_e(k'_{ex}, k'_{ey}, k'_{ez})$, where

$$k'_{ex} = \frac{d}{R}(n_e - n_o)\cos\varphi;$$

$$k'_{ey} = \frac{d}{R}(n_e - n_o)\sin\varphi; \quad k'_{ez} = \sqrt{1 - \frac{d^2}{R^2}(n_e - n_o)^2}. \tag{25}$$

As can be seen from (24) and (25), the partial e-beam falls on the point M from the beam entering CL-1 at a distance d from the axis:

$$d = \frac{R\rho_1}{(z - F_{ee})(n_e - n_o)}, \tag{26}$$

where $\rho_1 = \sqrt{x^2 + y^2}$.

The total amplitude when adding (oo) and (ee) beams depends on the phase difference $\Delta\psi$ between them:

$$\Delta\psi = \frac{2\pi(\Delta + (\overrightarrow{k_0} - \overrightarrow{k_e})\vec{r})}{\lambda}, \tag{27}$$

where $\overrightarrow{k_0}(0, 0, 1)$ is the unit vector of the o-beam and Δ is the path difference of o- and e-beams as they pass through the CL. It appears that Δ within the accuracy of up to $\left(\frac{d}{R}\right)^2$ (where d is the radius of the beam) does not depend on the position of the point $M(x, y, z)$ on the screen and is actually defined by the phase difference of o- and e-beams as they pass through the CL center. This result can be obtained through the consideration of beam trajectories.

The condition of the illumination maximum on the screen at the point $M(x, y, z)$ can be written as:

$$\Delta\psi = 2\pi S, \tag{28}$$

where $S = \pm 1; \pm 2; \pm 3.$

The substitution of (24) and (27) into (28) gives an equation of the locus of points of the illumination maximum on the screen:

$$(x^2 + y^2)\left[\frac{z}{2(z - F_{ee})^2}\right] = S\lambda - \Delta. \tag{29}$$

Equation (29) defines a clump of circles (Figure 4). Note that in

$$R_S = \frac{\sqrt{2S\lambda}(F_{ee} - Z)}{\sqrt{2F_{ee}} - Z}, \tag{30}$$

the tested CL, the value $\frac{\Delta}{\lambda}$ turned out to be very close to an integer; therefore the expression $S\lambda - \Delta$ in (29) may be replaced with $S'\lambda,$ where $S' = 0;$ $\pm 1; \pm 2,$ and the radii of the rings in the observed interference pattern are determined by the ratio:

Figure 4. The interference raster formed by the CL in the collimated laser beam/Fresnel zone pattern/in the context of interference between (oo) and (ee) waves. The analyzer $|A|$ is oriented at an angle 45º to $\vec{a}$.

Similarly, we obtain the expression for the interference of (oe) and (eo) waves at the CL output:

$$(x^2 + y^2)\left[\frac{z}{2(z - F_{ee})^2}\frac{1}{z - F_{ee}}\right] = S\lambda. \tag{31}$$

A similar interference pattern between (oo) and (ee) waves can also be obtained when changing the direction of incidence on the CL by 180°.

4. Conclusions

An original technique for calculating the path of laser radiation through a uniaxial crystalline lens has been developed. The expressions having high precisions describe the path of laser radiation through crystalline lenses and determine the conversion of different (ordinary and extraordinary) waves on the spherical surface of a crystalline lens elaborately. They are also suitable for engineering calculations. The equations which make it possible to determine the properties of crystalline lenses in the mode of splitting of polarized beams and interference between them as well as different cases of interference have been obtained and comprehensively studied. The conditions for the formation of interference of crystalline lenses with the help of the analyzer have been defined. The paper has also analyzed the prospects for the use of interference patterns generated by crystalline lenses in laser polarized interferometers.

Theoretically, the resulting expressions coincide with the experimental data to a high precision.

Acknowledgement

The authors thank the anonymous referees for their valuable suggestions towards the improvement of the manuscript.

References

[1] A. G. Arutyunyan, S. A. Akhmanov and Y. D. Golchev, Spatial correlation functions of the field and intensity of laser radiation, J. Exp. Theor. Phys. 64 (1973), 1511.

[2] B. Justh, Measurement of the spatial coherence of microdensitometer illumination, J. Exp. Theor. Phys. 65 (1973), 1789.

[3] F. T. S. Yu, Introduction to Diffraction, Information Processing and Holography, The MIT Press, London, 1973.

[4] R. J. Collier, C. B. Burkhardt and L. H. Lin, Optical Holography, Academic Press, New York, 1971.

[5] L. M. Soroko, Basics of Holography and Coherent Optics, Nauka, Moscow, 1971.

[6] D. Y. Galperin, Research on geometrical optics, Doctoral Dissertation, State Optical Institute, Leningrad, 1959.

[7] L. Cirkovic, D. E. Evans, M. J. Forrest and J. Katzenstein, Use of a birefringent plate to control the spectral emission of a ruby laser, App. Opt. 7(5) (1968), 981-982.

[8] Y. I. Ostrovskiy, Interference resolvometer, USSR Patent No. 207018, Bull. Invent. 9 (1968).

[9] M. Born and E. Wolf, Principles of Optics, Cambridge University Press, Cambridge, 1999.

[10] F. S. Landsberg, Optics, Nauka, Moscow, 1976.

[11] F. I. Fedorov and V. V. Filippov, Light Reflection and Refraction by Transparent Crystals, Nauka, Minsk, 1976.

[12] L. Csillag, M. Janossy and K. Kantor, Investigation of spatial coherence and phase change in the modes of a He-Ne laser, Phys. Lett. 20(6) (1966), 636-637.

[13] J. Svetlik, Simple methods for the measurement of laser beam parameters, Appl. Optics 13(6) (1974), 1276-1278.

[14] I. P. Shafranovsky, Optics, Publishing House of the USSR Academy of Sciences, Moscow, Leningrad, 1963.

[15] V. A. Osipov-King, Bifocal crystalline lens, USSR Patent No. 106823, Bull. Invent. 6 (1957).

[16] R. S. Eng and K. G. Leib, Multiple imagery with birefringent lenses, Appl. Opt. 8(10) (1969), 2117-2120.

[17] Y. V. Osipov, Polarizing lenses of binary structure, Opt. Mech. Ind. 5 (1973), 5-7.

[18] W. Kulcke, K. Kosanke, E. Max, H. Fleisher and T. J. Harris, Convergent beam digital light deflector, Optical and Electro-optical Information Processing, J. T. Tippett, D. A. Berkowitz, C. L. Clapp, C. J. Koester and A. Vanderburgh, Jr., eds., MIT Press, Cambridge, 1965.

[19] P. W. Smith, Mode selection in lasers, Proc. IEEE 60 (1972), 422-440.

[20] S. N. Bazykin, Optical schemes of informational-measuring systems based on laser interferometers, Mod. Probl. Science Ed. 1 (2015), 16-18.

[21] S. N. Bazykin, The measurement of angular displacements with the help of a laser acousto-optic interferometer, Proceedings of the International Symposium “Reliability and Quality”, Vol. 1, 2010.

[22] W. Demtroder, Laser spectroscopy: basic concepts and instrumentation, Vol. 5, Springer Series in Chemical Physics, Springer, Berlin, Heidelberg, 1981.

[23] M. Zhongsheng, Arbitrary vector beams with selective polarization states patterned by tailored polarizing films, Las. Phys. 23(10) (2013), 105-110.

[24] K. Hnatovsky, V. G. Shvedov, N. Shostka, A. V. Rode and W. Krolikowski, Polarization-dependent ablation of silicon using tightly focused femtosecond laser vortex pulses, Opt. Lett. 37 (2012), 226-228.

[25] I. Wang, Development and prospect of near field optical measurements and characterizations, Front Optoelectron. 5 (2012), 171-181.

[26] V. V. Kotlyar, Analysis of the shape of a sub wavelength focal spot for the linear by polarized light, Appl. Opt. 52 (2013), 330-339.

[27] S. N. Khonina, S. V. Karpeev, A. A. Morozov and V. D. Paranin, Implementation of ordinary and extraordinary beams interference by application of diffractive optical elements, J. Mod. Opt. 63(13) (2016), 1239-1247.
DOI: 10.1080/09500340.2015.1137368.

[28] S. N. Khonina, V. D. Paranin, S. V. Karpeev and A. A. Morozov, Study of polarization transformations and interaction of ordinary and extraordinary beams in nonparaxial regime, Comp. Opt. 38(4) (2014), 598-605.

[29] S. N. Khonina, S. V. Karpeev and S. V. Alferov, Theoretical and an experimental research of polarizing transformations in uniaxial crystals for generation cylindrical vector beams of high orders, Comp. Opt. 38(2) (2014), 171-180.

[30] S. N. Khonina, S. V. Karpeev, S. V. Alferov and V. A. Soifer, Generation of cylindrical vector beams of high orders using uniaxial crystals, J. Opt. 17 (2015), 065001–11 pp.

[31] V. D. Paranin, S. V. Karpeev and A. P. Krasnov, A converter of circularly polarized laser beams into cylindrical vector beams based on anisotropic crystals, Comp. Opt. 39(5) (2015), 644-653.

[32] S. V. Alferov, S. N. Khonina and S. V. Karpeev, Study of polarization properties of fiber-optics probes with use of a binary phase plate, J. Opt. Soc. Amer. 31(4) (2014), 802-807.

[33] V. D. Paranin, S. V. Karpeev and S. N. Khonina, Control of the formation of vortex Bessel beams in uniaxial crystals by varying the beam divergence, Quantum Electronics 46(2) (2016), 163-168. DOI: 10.1070/QEL15880.

[34] S. V. Alferov, S. V. Karpeev, S. N. Khonina and O. Y. Moiseev, Experimental study of focusing of inhomogeneously polarized beams generated using sector polarizing plates, Comp. Opt. 38(1) (2014), 57-64.

[35] K. Venkatakrishnan, Generation of radically polarized beam for laser micromachining, J. Las. Micr. Nanoeng. 7(3) (2012), 274-278.